Engineering Structures 179 (2019) 556–565

Contents lists available at ScienceDirect

Engineering Structures

journal homepage: www.elsevier.com/locate/engstruct

Accelerated optimization method for low-embodied energy concrete box-girder bridge design

Vicent Penadés-Plà[a], Tatiana García-Segura[b,*], Víctor Yepes[a]

[a] Institute of Concrete Science and Technology (ICITECH), Universitat Politècnica de València, 46022 Valencia, Spain
[b] School of Civil Engineering, Universitat Politècnica de València, 46022 Valencia, Spain

ARTICLE INFO

Keywords:
Low-embodied energy
Post-tensioned concrete
Box-girder bridge
Structural optimization
Metamodel
Kriging

ABSTRACT

Structural optimization is normally carried out by means of conventional heuristic optimization due to the complexity of the structural problems. However, the conventional heuristic optimization still consumes a large amount of time. The use of metamodels helps to reduce the computational cost of the optimization and, along these lines, kriging-based heuristic optimization is presented as an alternative to carry out an accelerated optimization of complex problems. In this work, conventional heuristic optimization and kriging-based heuristic optimization will be applied to reach the optimal solution of a continuous box-girder pedestrian bridge of three spans with a low embodied energy. For this purpose, different penalizations and different initial sample sizes will be studied and compared. This work shows that kriging-based heuristic optimization provides results close to those of conventional heuristic optimization using less time. For the sample size of 50, the best solution differs about 2.54% compared to the conventional heuristic optimization, and reduces the computational cost by 99.06%. Therefore, the use of a kriging model in structural design problems offers a new means of solving certain structural problems that require a very high computational cost and reduces the difficulty of other problems.

1. Introduction

The traditional main objective of structural engineering is to reach maximum safety with the minimum investment. However nowadays, due to the increased concern for sustainability, other aspects have also become important within the field of structural engineering. These aspects are usually grouped into the three main objectives (economic, environmental and social) of sustainability [1,2]. In this way, the traditional structural engineering problem becomes a complex problem that should be solved by means of a decision-making process [3,4]. Regarding the environmental goal, life-cycle assessment is an accepted process to obtain the complete environmental profile of a process, product or service [5–7]. However, a first approximation of the environmental assessment can be carried out using a single criterion that represents, in a reliable way, the environmental impact. The most representative criteria are the CO_2 emissions and the embodied energy, which also have a direct relationship with the cost [8,9]. This indicates that the optimization of CO_2 emissions or embodied energy reduces at the same time the cost. There are several works that have analyzed structures with a lower CO_2 emission [10,11], but the embodied energy has been less studied [12].

Bridges are one of the most important structures in civil engineering due to their importance in the area of communications. However, designing a sustainable bridge is not easy, due to the fact that the structural problem is characterized by a large number of design variables with multiple combinations. A heuristic optimization process is presented as an alternative to achieve a solution within the design space that reaches the objectives and guarantees the constraints imposed by the regulations. This method has been used to optimize many types of structures, such as reinforced concrete columns [13,14], reinforced concrete frames [8], precast concrete floors [15], prestressed concrete precast road bridges [12] and post-tensioned concrete box-girder bridges [11,16]. However, the structural optimization problem depends on a large number of design variables with several constraints. This results in excessive computational costs [17]. One effective solution to carry out the optimization with a lower computational cost is the use of approximate response surfaces obtained by surrogate models or metamodels. The most common metamodels are polynomial regression, neural networks and kriging [18,19]. The kriging model is one of the most encouraging metamodels used in structural optimization [20] although despite this fact, only few works have been carried out using a kriging-based heuristic optimization to design real structures. This model provides an optimal interpolation based on regression against observed values of the surrounding data points, weighted according to

* Corresponding author.
E-mail addresses: vipepl2@cam.upv.es (V. Penadés-Plà), tagarse@upv.es (T. García-Segura), vyepesp@cst.upv.es (V. Yepes).

https://doi.org/10.1016/j.engstruct.2018.11.015
Received 11 June 2018; Received in revised form 3 October 2018; Accepted 7 November 2018

spatial covariance values. This means that kriging considers both global and local approximations at the same time. Thus, the kriging model takes into account the local variations of the objective response. In this context, a methodology that allows optimal designs to be determined with adequate accuracy and at reduced time cost is highly desirable.

In this work, conventional heuristic optimization and kriging-based heuristic optimization will be applied to determine an optimized continuous box-girder pedestrian bridge of three spans with a low embodied energy. A comparison between both optimization techniques will be carried out to determine if the kriging-based heuristic optimization provides reasonable results compared with the conventional heuristic optimization. For this purpose, different coefficients of penalizations and sampling sizes will be considered to determine the characteristics of the kriging-based heuristic that performs better. After that, a set of parameters for the kriging model will be recommended. In Section 2 both optimization processes will be described. In Section 3, a general scheme of the process to construct a metamodel will be shown, focusing on the main methods used in this work, namely latin hypercube sampling and the kriging model. In Section 4, the problem design will be described, and in Section 5 the most important results will be shown. Finally, the most important conclusions will be detailed.

2. Optimization process

Optimization is a process that tries to find the best possible solution to a problem that may be defined by one (mono-objective) or several (multi-objective) objective functions, f, that satisfy some constraints, g_j.

$$f(X) \tag{1}$$

$$g_j(X) \leq 0 \tag{2}$$

where X represents the vector with the design variables chosen for the formulation.

The optimization process is defined by the algorithm used and establishes a set of rules to be followed in solving operational problems. These algorithms can be divided into exact algorithms and heuristic algorithms. Exact algorithms reach the global optimum by using sequential techniques of mathematical programming. Heuristic algorithms were developed to solve complex and realistic structural optimization problems of discrete variables. These algorithms achieve good solutions without guaranteeing the global optimum, but with a lower computational cost. Complex optimization problems, such as structural optimization, are defined for a large number of design variables, and thus the heuristic algorithms have demonstrated the best behavior in solving this kind of problem.

Heuristic algorithms try to simulate simple events observed in nature. In general, the traditional heuristic algorithms look for a local optimum, while the metaheuristic algorithms have tools to avoid local optimums in order to find a better solution. Metaheuristic algorithms follow an iterative process in which a complete structural design (combination of design variables) is defined to carry out the structural analysis and to evaluate aptitude by an objective function (Fig. 1). In recent years, some metaheurisitc algorithms have been applied to structural optimization including the variable neighborhood search [10], harmony search [21], threshold function [22], memetic algorithm [23], glowworm swarm algorithm [9] and simulated annealing [11] among others.

However, despite the advances in technology, the computational cost of structural heuristic optimization is still very high [24] due to the finite element structural analysis carried out during all iterations of the optimization process. This high computational cost can be reduced by means of metamodels (also called surrogate models or approximation models) [17]. These metamodels construct a mathematically approximate model of the objective function from a set of points in the design space (initial sampling) to predict the output without the need to carry out a full structural analysis. This means that the slowest part of the process of conventional heuristic optimization, which is the structural analysis and evaluation of the objective function part, is replaced by an evaluation of the metamodel. Therefore, the computational cost necessary for metamodel-based heuristic optimization (Fig. 2) is lower than the computational cost necessary for conventional heuristic optimization.

3. Metamodel construction process

The basis of metamodels consists of constructing an approximate mathematical model of a detailed simulation model, which predicts the output data (objective response) from input data (design variables) in the whole design space, more efficiently than the detailed simulation models. It could, as such, be called a model of the model. The construction process of a metamodel focuses on three main parts: (a) obtaining the initial input dataset points inside the design space, (b) choosing the metamodel type to construct the approximate mathematical model and (c) choosing the fitting model. There are a large number of options for carrying out these steps [25]. Regardless of the choice for each step, the main objective of constructing a metamodel is to obtain a model with the best accuracy possible to predict the objective response.

The choice of the initial input dataset points or sampling inside the design space is defined by the sample size and the position of the points, because both aspects have an influence on the model construction. On the one hand, the sample size is fundamentally related to the number of design variables. The sample size must be higher with a larger number of design variables for the same accuracy of the metamodel, and therefore the computational cost necessary to construct the model will be higher. On the other hand, once the sample size has been defined, the position of the points must be placed within the design space in order to obtain the best possible information. This process is called *Design Of Experiments (DoE)*.

The DoE can be divided into two different groups. The first group clusters the classic designs, that include the *factorial* or *fractional factorial designs*, *central composite designs*, *Box-Behnken designs*, *Plackett-Burman designs*, *Koshal designs* and *D-optimal designs* [26]. These types of designs tend to spread the sample points around the border of the design space and only include a few points inside of it. The classic designs are mainly used to construct polynomial metamodels. When the initial input data points were used to construct more advanced metamodels, other designs, called space-filling designs, were preferred. These types of designs trend to spread the sample points all over the design space (often with a uniform distribution), so it is possible to take into account the local phenomena in any region of the design space. The most popular space-filling designs are latin hypercube sampling [27], distance-based designs [28] and low-discrepancy sequences, which group Hammersley sequence sampling [29] and the uniform design [30].

In this work, to generate the sample, latin hypercube sampling (LHS) has been considered; its effectiveness in the estimation of the objective response of the metamodel has been proven in several works [31,32]. LHS was proposed by McKay et al. in 1979 [27]. This method determines the N number of non-overlapping intervals for each variable (in this work these intervals are divided according to a uniform distribution) from a number of design variables (v) and a number of initial input dataset points (N). Therefore, the design space is divided into N^v regions. Each sample point will be located in one region in order that each point corresponds to a combination of different intervals of each design variable range. In this way, each interval of each design variable range will only be associated with one sample point. Consequently, the LHS guarantees that all of the design variables are represented along their respective ranges. Fig. 3 shows an example with 2 design variables and 10 initial input dataset points.

Once the sample is defined, the objective response of the initial input dataset points is obtained. All of this initial information (inputs and outputs) is used to construct the metamodel over all of the design space. In this way, the metamodel predicts the objective response

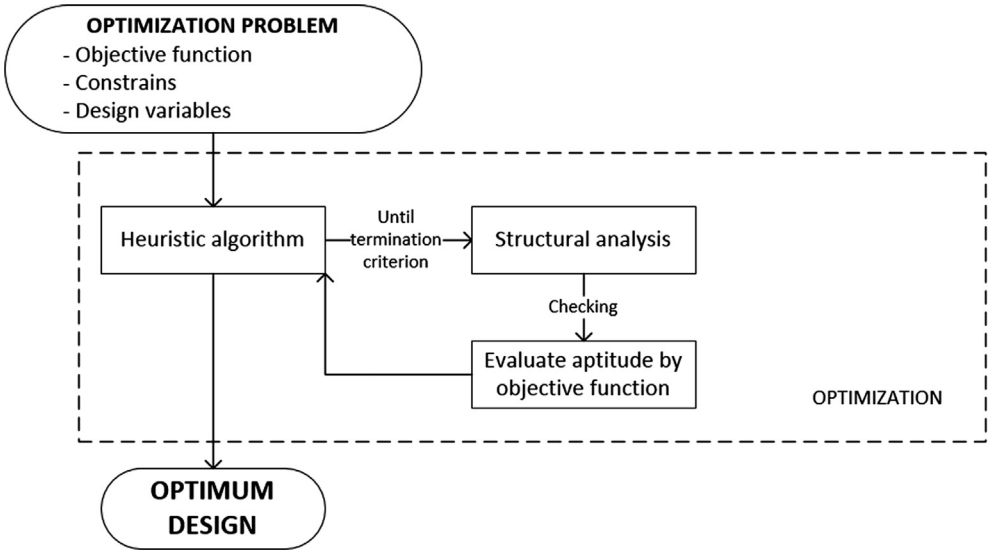

Fig. 1. General flow chart of conventional heuristic optimization process.

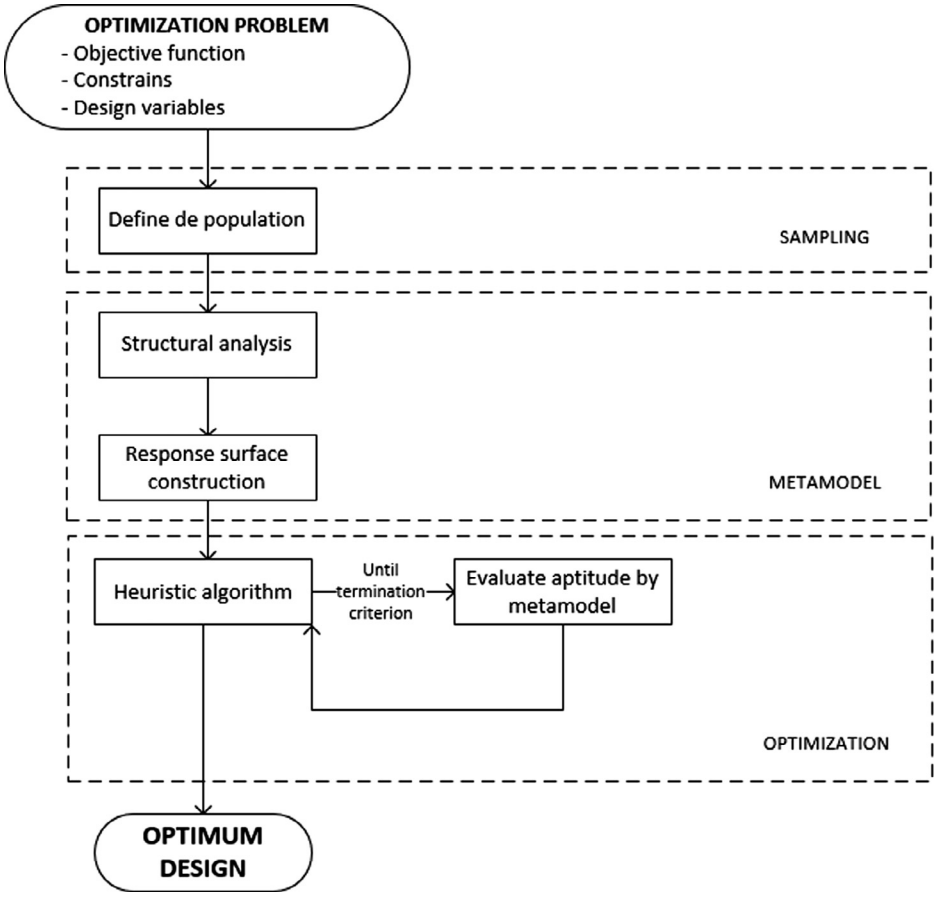

Fig. 2. General flow chart of metamodel-based heuristic optimization.

according to a mathematical function:

$$y = f(x) = g(x) + \varepsilon \tag{3}$$

where x are the input dataset points, $f(x)$ corresponds to the real response (model), $g(x)$ represents the approximate response (metamodel) and ε represents the approximation error. There are several mathematical formulations to construct metamodels with different characteristics [19,25]. Although these metamodels have been compared [32–34], it is not possible to determine if one is better than the others as this depends on the problem posed. However, the most common metamodels are polynomial regression, neural networks and kriging [18,19]. The polynomial-based response surface model is sometimes difficult to use in complex engineering problems, and the neural network-based model requires many sample points and much computational time for the training of the network [35]. The kriging model is a promising metamodel as it is more flexible than polynomial-based models and less time consuming than neural network-based techniques [33]. Thus, this work uses the kriging formulation to

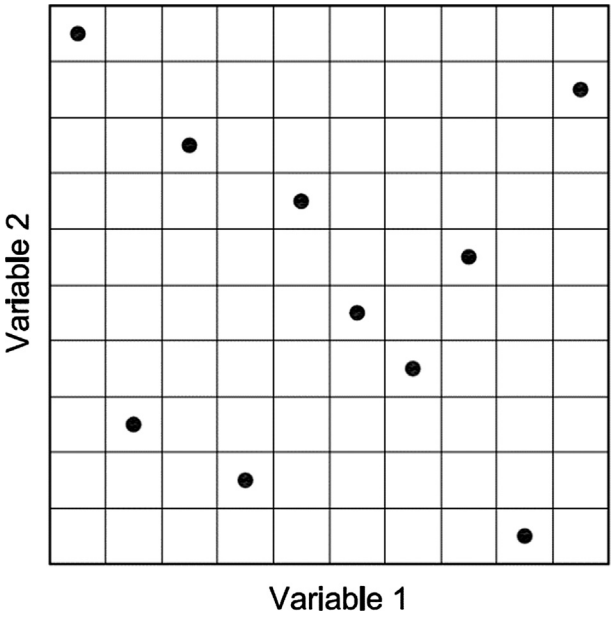

Fig. 3. Latin hypercube sampling (v = 2 and n = 10).

construct the metamodel.

Kriging is a metamodel that has its origins in geostatic applications involving spatially and temporally correlated data and was developed by the South African mining engineer called Danie Gerhardus Kirge. Later, many researches contributed to the problem of optimal spatial prediction, but the approach was formalized by Matheron in 1963 [36] who used the term kriging in honor of the contribution of Danie Gerhardus Kirge [20]. The idea behind kriging is that the deterministic response $y(x)$ can be described as:

$$y(x) = f(x) + Z(x) \tag{4}$$

where $f(x)$ is the known approximation function, and $Z(x)$ is a realization of a stochastic process with mean zero, variance σ^2 and non-zero covariance. The first term of the equation, $f(x)$, is similar to a regression model that provides a global approximation of the design space (Eq. (5)). The second term, $Z(x)$, creates local deviations so that the kriging model interpolates the initial sample points (Eq. (6)). In many cases, $f(x)$ is simply a constant term and the method is then called ordinary kriging. If f(x) is set to 0, implying that the response $y(x)$ has a mean of zero, the method is called simple kriging [37].

$$f(x) = \sum_{i=1}^{n} \beta_i \cdot f_i(x) \tag{5}$$

$$cov[Z(x_i), Z(x_j)] = \sigma^2 \cdot R(x_i, x_j) \tag{6}$$

where the process variance σ^2 scales the spatial correlation function $R(x_i, x_j)$ between two data points. In engineering design, the Gaussian correlation function (Eq. (7)) is the most commonly used [37] function that can be defined with only one parameter (θ) that controls the area of influence of nearby points [35]. A low θ means that all the sample points have a high correlation, thus the term $Z(x)$ will be similar all over the design space. As the value θ increases, the points with higher correlation will be closer, thus the term $Z(x)$ will differ depending on the point in the design space:

$$R(x_i, x_j) = e^{-\sum_{k=1}^{m} \theta |x_k^i - x_k^j|^2} \tag{7}$$

Finally, each metamodel type has its associated fitting method. In this case, the kriging formulation uses the search for the Best Linear Unbiased Predictor (BLUP). Simpson et al. [19] gave a detailed review of the equations and fitting methods for common metamodel types.

4. Problem design

In this section, a comparison of conventional heuristic optimization and kriging-based heuristic optimization will be discussed. First of all, the structure considered (a continuous concrete box-girder pedestrian bridge) and all of the characteristics involved will be described. After that, the optimization problem associated with the bridge will be defined. Finally, both optimization processes will be explained. This final point includes the design variables considered in each case, as well as how each approach deals with the constraints.

4.1. Box-girder pedestrian bridge description

The bridge is a continuous concrete box-girder pedestrian bridge deck with three continuous spans of 40–50–40 m length (the relationship between the external span and the central span follows the optimum of 80%). This type of bridge is commonly used due to its structural performance, low dead load and construction conditions. The pedestrian bridge deck has a constant width of 3 m, and the remaining geometrical dimensions of the cross-section are defined by the seven variables of (Fig. 4): depth (h), bottom slab width (b), web inclination width (d), top slab thickness (es), external cantilever section thickness (ev), bottom slab thickness (ei) and webs slab thickness (ea). The value of these variables is limited for a range. The depth range is 1.25–2.5 m, the bottom slab width range is 1.2–1.8 m, the width of the web inclination range is 0–0.4 m, the web slab thickens is 0.3–0.6 m and the other slab thickness ranges are 0.15–0.4 m. The haunch (t), is calculated from the values of other variables (Eq. (8)) according to Schlaich and Scheff's [38] recommendation. In addition, the haunch must provide the space to contain the ducts in the high and low points.

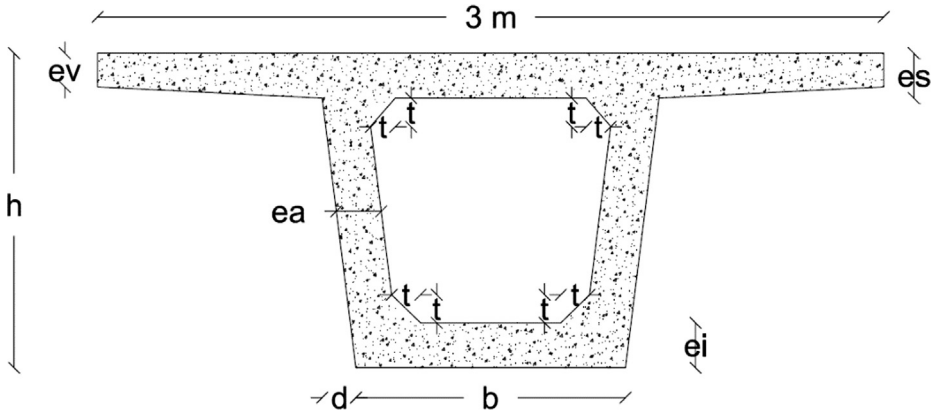

Fig. 4. Box-girder cross-section.

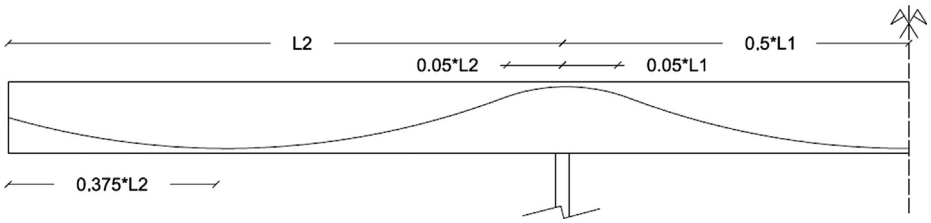

Fig. 5. Pedestrian bridge and duct layout.

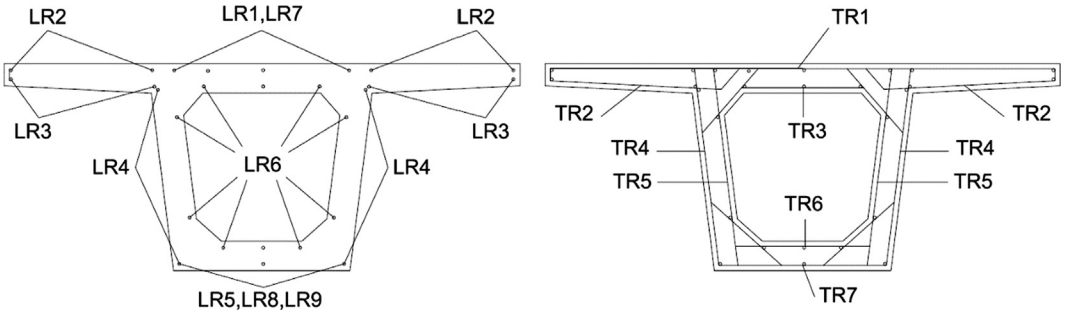

Fig. 6. Longitudinal and transversal reinforcing steel disposition.

$$t = \max\left\{\frac{b - 2{\cdot}ea}{5}, ei\right\}. \quad (8)$$

The strength of the concrete is defined by the variable f_{ck} that can take a value inside of the range 35–100 MPa. The post-tensioned steel formed by 0.6 in. strands is prestressed to 195.52 kN. The ducts are symmetrically distributed through the webs with a parabolic layout. The maximum eccentricity is present where the bending moment is the maximum or minimum (Fig. 5). At these points, the distance considered between the duct and the surface is 0.2 m. The distance from the piers to the point of inflection is defined by 5% of the length of each span. In addition, the position of the reinforced steel is defined according the Fig. 6. Longitudinal reinforcement is defined by the number of bars per meter and their diameter, placed at the top slab (LR_{n1}, $LR\emptyset_1$), the flange (LR_{n2}, $LR\emptyset_2$, LR_{n3}, $LR\emptyset_3$), the web (LR_{n4}, $LR\emptyset_4$), the bottom slab (LR_{n5}, $LR\emptyset_5$) and the core (LR_{n6}, $LR\emptyset_6$). In addition, extra bending reinforcement is divided into two systems. One covers the top slab at the support zone (L/5 on both sides of the piers), with a diameter defined by $LR\emptyset_7$ and the same number of bars per meter as LR_{n1}. The other is placed at the bottom slab throughout the rest of the external span ($LR\emptyset_8$) and the central span ($LR\emptyset_9$). The number of bars per meter is, for both locations, equal to LR_{n5}. The diameter can change according to 0, 10, 12, 16, 20, 25 and 32 mm. Regarding transverse reinforcement, the diameter of the standard reinforcement ($TR\emptyset_1$, $TR\emptyset_2$, $TR\emptyset_3$, $TR\emptyset_4$, $TR\emptyset_5$, $TR\emptyset_6$, $TR\emptyset_7$) is set with the same spacing (TRS) for construction requirements.

Traditional scaffolding is used in the construction stage with a clearance of 5 m. The formwork is disposed over the scaffolding to give the shape of the cross section of the bridge. In addition, lighting is used to lighten the self-weight of the bridge. Table 1 defines the other conditions employed in this study such as the materials, the load actions on the structure, the exposure class and the regulations used.

4.2. Optimization problem description

In this work, the problem of continuous concrete box-girder pedestrian bridge deck optimization involves a single-objective optimization of the embodied energy of the structure. Hence, this optimization aims to minimize the embodied energy (Eq. (9)) and satisfy the constraints (Eq. (10)).

$$Embodied\ \ energy = \sum_{i=1,n} e_i \times m_i(x_1, x_2, \cdots, x_n) \quad (9)$$

Table 1
Main parameters of the analysis.

Material parameters	
Maximum aggregate size	20 mm
Reinforcing steel	B-500-S
Post-tensioned steel	Y1860-S7
Strand diameter	$\Phi_s = 0.6''$
Tensioning time	7 days
Geometrical parameters	
Pedestrian bridge width	B = 3 m
Number of spans	3
Central span length	L1 = 50 m
External span length	L2 = 40 m
Clearance	5 m
Diaphragm thickness	1.2 m
Exposure related parameters	
External ambient conditions	IIb
Regulation related parameters	
Regulations	EHE-08/IAP-11/Eurocodes
Service working life	100 years
Loading related parameters	
Reinforced concrete self-weight	25 kN/m^3
Asphalt layer self-weight	24 kN/m^3
Mean asphalt thickness	47.5 mm
Bridge railing self-weight	1 kN/m
Live load	5 kN/m^2
Differential settling	5 mm

$$g_j(x_1, x_2, x_3, \cdots, x_n) \leq 0 \quad (10)$$

where x_1, x_2, x_3, .., x_n are the design variables.

The objective function evaluates the embodied energy for the total number of construction units considering the material used and the placement embodied energy defined in Eq. (9). The embodied energy of each unit (e_i), shown in Table 2, were obtained from the BEDEC ITEC database [39]. The embodied energy of concrete is determined for each compressive strength grade according to the mix design, including the embodied energy of raw materials extraction, manufacture and transportation. The measurements (m_i) concerning the construction units are evaluated from the design defined using the design variables.

The structural constraints represented by Eq. (10) check the serviceability and ultimate limit states (SLS and ULS) of Vertical shear, Longitudinal shear, Punching shear, Bending, Torsion, Torsion combined with bending and shear, Cracking, compression and tension

Table 2
Unit energy.

Unit measurements	Energy (kWh)
m^3 of scaffolding	20.4
m^2 of formwork	8.7
m^3 of lighting	1137.5
kg of steel (B-500-S)	10.44
kg of post-tensioned steel (Y1860-S7)	12.99
m^3 of concrete HP-35	612.22
m^3 of concrete HP-40	646.61
m^3 of concrete HP-45	681
m^3 of concrete HP-50	715.39
m^3 of concrete HP-55	749.77
m^3 of concrete HP-60	784.16
m^3 of concrete HP-70	852.94
m^3 of concrete HP-80	921.72
m^3 of concrete HP-90	990.49
m^3 of concrete HP-100	1059.27

stress, vibration. Note that the code [40] provides different equations for conventional and high-strength concrete (concrete with a characteristic compressive strength greater than 50 MPa). In addition, the geometrical and constructability requirements are verified, following the Spanish regulations for this type of structure [40,41] as well as the Eurocodes [42,43]. It is worth mentioning that the analysis and the verification of the limit states are coded in Matlab.

The algorithm used to carry out the optimization problem is simulated annealing (SA) [44] due to its versatile acceptance criterion. Many works use SA to carry out conventional heuristic optimization [8,45]. In this work, the initial temperature is calibrated following Medina's [46] method, which proposes that the initial temperature is halved when the percentage of acceptances is greater than 40%, and doubled when it is less than 20%. After that, the temperature decreases according to a coefficient of cooling k following the equation $T = k * T$, when a Markov chain ends. In this work, the calibration revealed that a coefficient of cooling of 0.8 and a length of the Markov chain of 1000 are appropriate. The algorithm finishes after three Markov chains show no improvement.

4.3. Optimization process

As stated above, in this work, a comparison between conventional heuristic optimization and kriging-based optimization will be carried out. The main difference between these processes is that, while in conventional heuristic optimization, before obtaining the objective response, all of the constraints of the bridge are checked at each step of the optimization, in kriging-based heuristic optimization, the objective response is estimate throughout a mathematical approximation.

4.3.1. Conventional heuristic optimization

In conventional optimization, in addition to the seven geometrical variables and the concrete strength, the reinforced steel and the prestressed steel are also variables. Reinforced steel is defined by 23 variables, 15 for the longitudinal reinforcement and 8 for the transverse reinforcement (see Fig. 6). Once the initial box-girder pedestrian bridge is completely defined, the SA algorithm carries out movements of the design variables to compare the objective response obtained after each movement until the energy-optimized box-girder pedestrian bridge is reached according to the process defined in Section 2. Each movement requires the complete verification of the SLS and ULS, entailing a high computational cost. Fig. 2 shows a scheme of the conventional heuristic optimization considered.

4.3.2. Kriging-based heuristic optimization

In contrast to the conventional heuristic optimization in which the bridge is defined completely at the beginning of each iteration to later verify all of the constraint defined by the regulations, kriging-based heuristic optimization only defines the design variables that the engineers would take into account in their design (geometrical variables and the concrete strength) to later calculate the amount of the post-tensioned steel and the reinforced steel required according to the standards. Therefore, the post-tensioned and reinforced steel are not variables, and consequently, the design space is greatly reduced.

First of all, a specific sample size (N) over all the design space is obtained according to LHS, then, the embodied energy is calculated for each of these points. Due to the complexity of structural problems, there are regions of the design space for which certain combinations of the geometrical design variables are not possible (for example $h < es + ev + 2 * t$). This is because the embodied energy of the bridge cannot be obtained in some points of the LHS. To solve this constraint and attempt to conduct the optimization for feasible designs, two response surfaces will be constructed. The first one is determined by the feasible solutions of the LHS. With this response surface, the objective response of the unfeasible solutions of the LHS will be estimated and a penalization is applied to those solutions. To prevent too much skewing of the response surface, the penalization is imposed depending on the case: if the total embodied energy is higher than the minimum embodied energy of the set of feasible solutions, the embodied energy is not modified (case 1). Otherwise, if the total embodied energy is lower than the minimum embodied energy of the set of feasible solutions, a penalization is imposed to avoid reaching unfeasible optimum solutions (case 2). A study of the penalization imposed will be carry out in the next section. Finally, on grouping all of the feasible and non-feasible solutions, a second response surface will be determined. This response surface is constructed considering all of the LHS points, and thus all of the design space will be represented. In addition, the penalization avoids the optimization tending towards to unfeasible solutions.

Once the final response surface is obtained, a validation process that compares the real embodied energy and the estimated embodied energy of nine random data points is carried out in order to determine the accuracy of the model. Then, heuristic optimization by means of the SA algorithm is carried out to determine the final energy-optimized continuous concrete box-girder pedestrian bridge. Finally, the estimated optimized solution will be checked. In the case that this solution is feasible, the process finishes, but if the solution is unfeasible, a new initial population by LHS will be generated and the entire process is repeated. This procedure aims to study the influence of the initial population (N) on the accuracy of the model, the optimization and the computational cost. Fig. 7 shows the scheme followed in this kriging-based heuristic optimization.

5. Results

In this section, the results of the comparison between conventional heuristic optimization and kriging-based heuristic optimization are shown. For this purpose two main objectives are proposed in this study: (1) to obtain the characteristics of the kriging model that provides good results of the optimization process, and (2) to study if the kriging-based heuristic optimization reaches acceptable results compared with the conventional heuristic optimization. The comparative study is carried out based on the mean results and best result of nine optimized solutions.

Before comparing the optimization methodologies, a sensitivity study is carried out to study the coefficient of penalization (p) applied to the unfeasible solutions of case 2. Different p values have been considered including 1, 1.25 and 1.5, and applied to the highest population considered ($N = 500$) in order to determine the influence of this parameter on the kriging model. Table 3 shows the results of a group of nine solutions for each different coefficient of penalization. The first three columns refer to the mean results and the last one to the best result of each group. The first column shows the accuracy of the kriging model, evaluated as the mean difference of the real embodied

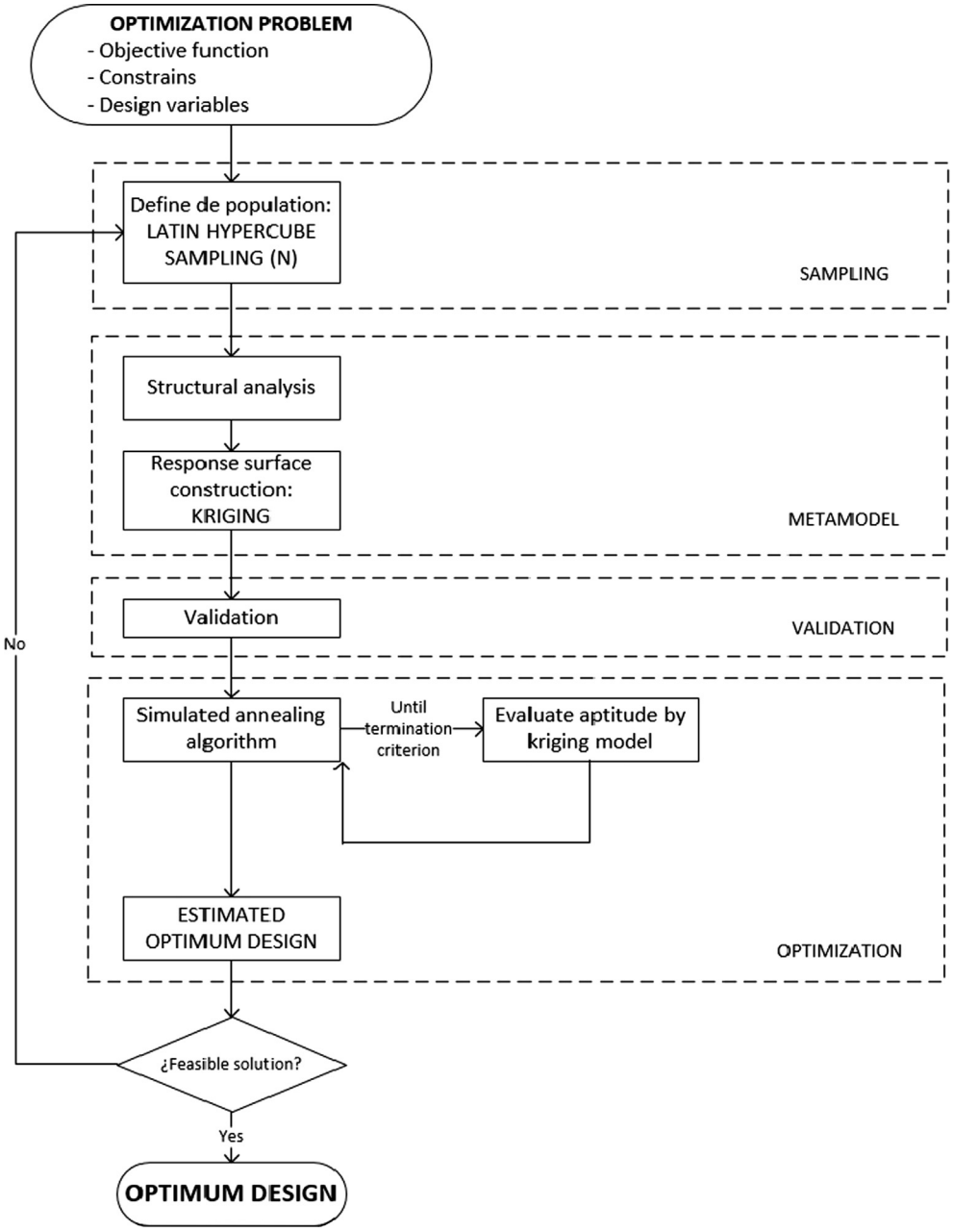

Fig. 7. Kriging-based heuristic optimization.

Table 3
Study of coefficient of penalization.

	Mean results			Best result
	Surface accuracy (%)	Embodied energy (kWh)	Optimized-solutions accuracy (%)	Embodied energy (kWh)
p = 1	3.88%	744,156	4.01%	701,910
p = 1.25	3.52%	750,254	4.83%	704,500
p = 1.5	3.99%	771,853	4.58%	731,210

energy and the estimated embodied energy of nine random points. The second and third columns show the mean embodied energy of nine optimized solutions in kWh and the accuracy of these nine optimized solutions. Finally, the last column shows the best optimized solution in kWh. Both the mean embodied energy and the best embodied energy improve when the coefficient of penalization decreases. For example, the mean embodied energy decreases from 771,853 kWh to 744,156 kWh when the coefficient of penalization decreases from 1.5 to 1. It shows that considering a coefficient of penalization of one improves the following optimization. This demonstrates that the kriging surface has a better behavior when there are smaller variations in its objective response. Thus, the coefficient of penalization considered to carry out this study will be $p = 1$.

Once the coefficient of penalization is determined, nine kriging surfaces are obtained for each initial sample size ($N = 10$, $N = 20$, $N = 50$, $N = 100$, $N = 200$, $N = 500$) to evaluate the influence of the sample size on the accuracy of the results. The accuracy of this kriging surface is evaluated through the mean of the difference between the real embodied energy and the predicted embodied energy of a random sample of the design space. Fig. 8 shows that the accuracy of the kriging surface increases with the number of initial samples but a horizontal convergence is observed from $N = 50$, in which the accuracy of the surface is 4.04%. From N = 10 to N = 50 the accuracy of the kriging

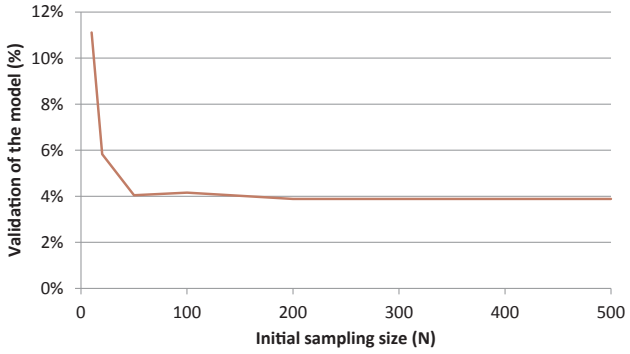

Fig. 8. Validation of kriging response surface.

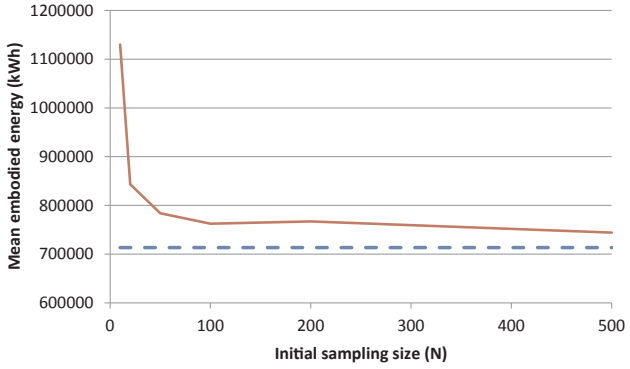

Fig. 9. Comparison of the mean of embodied energy of bridges.

model improves from 11.11% to 4.04% (upgrading of 7.07%). However, the accuracy of the kriging model from $N = 50$ to $N = 500$ improves from 4.04% to 3.88% (upgrading of only 0.16%).

Once the kriging surface is obtained, the optimization is carried out. For each initial sample size, different characteristics of the two optimizations have been compared. Fig. 9 shows the mean embodied energy of nine optimized box-girder pedestrian bridges. The horizontal dashed line represents the mean embodied energy obtained by conventional heuristic optimization, while the solid line represents the mean embodied energy obtained by the kriging-based heuristic optimization according to the sample size. The mean embodied energy of the nine optimized bridges obtained by the conventional heuristic optimization is 713,504 kWh. This result improves by 4.30% the best mean embodied energy of the nine optimized bridges obtained by the kriging-based heuristic optimization (corresponding to $N = 500$). Furthermore, as can be seen in Table 4, the best solutions of each group of nine obtained by kriging-based heuristic optimization are close to the best solution of the conventional heuristic optimization. For example,

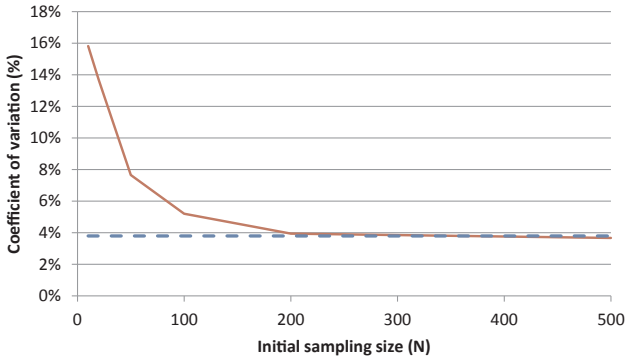

Fig. 10. Comparison of the coefficient of validation.

the best solution obtained with $N = 50$ differs only 2.54% with respect to the best solution of the conventional heuristic optimization. Besides, Fig. 10 shows that the increment in the initial sample size reduces the coefficient of variance of the nine solutions, reaching a lower value than the coefficient of variance of the nine solutions obtained in the conventional heuristic optimization. While the coefficient of variance of the conventional heuristic optimization is 3.79%, the coefficient of variance of the kriging-based heuristic optimization is 3.67% when the sample size is N = 500. These results show that a satisfactory solution can be obtained with an initial sample size of $N = 50$, but a higher initial sample size improves the accuracy of the model and the mean embodied energy. Thus, it can be said that the kriging model is robust for optimization problems.

It must not be forgotten that the main advantage of the kriging-based heuristic optimization is the computational cost saving as the objective response of each iteration is directly obtained. The kriging-based heuristic optimization required 1804.11 s for an initial sample size of $N = 500$, while the conventional heuristic optimization required 19617.14 s. This is a reduction of 90.80% in the computational cost. Note that the greater part of the computing time in the kriging-based heuristic optimization is due to the generation of the initial population. Regarding the conventional heuristic optimization, more than 80% of the computing time is spent in the analysis and the verification of the ultimate and serviceability limit states, as well as the geometrical and constructability requirements. Table 4 shows in more detail the time savings achieved for the other initial sample sizes.

Table 4 summarizes the most important results in comparing the optimization approaches. The first six rows represent the different initial sample sizes of the kriging-based heuristic optimizations, and the last row represents the conventional heuristic optimization. The columns represent the results of the different characteristics studied. The first six columns show the main results of the nine optimized bridges, and the last two columns show the best optimized bridges for each case. The first column shows the accuracy of the kriging model, evaluated as

Table 4
Overview of results obtained.

Method	N	Mean results						Best result	
		Surface accuracy (%)	Time (s)	Time comparison with CH (%)	Embodied energy (kWh)	Energy comparison with CH (%)	Coefficient of variance (%)	Embodied energy (kWh)	Comparison with CH (%)
Kriging-based heuristic optimization (KH)	10	11.11%	26.73	99.86%	1,130,127	58.39%	15.81%	814,840	19.49%
	20	5.83%	236.71	98.79%	844,816	18.2%	13.67%	721,400	5.79%
	50	4.04%	185.08	99.06%	783,726	9.84%	6.65%	699,240	2.54%
	100	4.16%	510.10	97.40%	762,350	6.85%	5.20%	700,800	2.77%
	200	3.88%	1497.33	92.37%	767,034	7.50%	3.94%	701,910	2.93%
	500	3.88%	1804.11	90.80%	744,157	4.30%	3.67%	701,910	2.93%
Conventional heuristic optimization (CH)			19617.14		713,505		3.79%	681,917	

the mean difference of the real embodied energy and the estimated embodied energy of nine random points. The second and third columns show the mean computational time of nine optimized solutions in seconds and the percentage with respect to the conventional heuristic optimization. The fourth and fifth columns show the mean embodied energy of nine optimized solutions in kWh and the percentage with respect to the conventional heuristic optimization. The sixth column shows the coefficient of variance of the nine optimized solutions. Finally, the seventh and eighth columns show the best optimized solution of each group of nine in kWh and the percentage with respect to the conventional heuristic optimization. This table can be used as a reference for defining the initial sample size. Note that the design space of this work is formed by 8 variables. Depending on the preferred characteristics, one sample size will be adjusted more than the others. However, taking into account all of the characteristics, the initial sample size that shows the best behavior is $N = 50$. This initial sample size provides a satisfying mean embodied energy (783,726 kWh) with a low coefficient of variance (6.65%) and gives the best solution (699,240 kWh) whose cross section variables are $b = 1.2$ m, $h = 1.35$ m, $d = 0$ m, $e_v = 0.15$ m, $e_s = 0.15$ m, $e_a = 0.35$ m, $e_i = 0.15$ m, and $f_{ck} = 60$ MPa. These results have been obtained with a 99.06% reduction in time spent with respect to the conventional heuristic optimization, whose cross section variables are $b = 1.35$ m, $h = 1.3$ m, $d = 0$ m, $e_v = 0.15$ m, $e_s = 0.2$ m, $e_a = 0.4$ m, $e_i = 0.2$ m, and $f_{ck} = 50$ MPa. In addition, Figs. 8–10 show that the initial sample size of $N = 50$ is close to the results of $N = 500$, but saving 89.74% of the computational cost. However, as mentioned previously, the sample size of $N = 500$ improves the coefficient of variance.

6. Conclusions

In this work, a conventional heuristic optimization and a kriging-based heuristic optimization have been compared. The results show that the use of the kriging model provides a response surface with a goof accuracy that improves with an increase in the initial sample size. Therefore, the objective response of a problem can be obtained without any structural analysis and with a high accuracy. The results of kriging-based heuristic optimization are close to the solutions reached in the conventional heuristic optimization cases with a significantly high reduction of computational cost.

The sensitivity analysis of the penalization imposed on the unfeasible designs shows that the kriging model has a better behavior with the lowest penalization. In addition, the study of the optimization obtained according to the initial sample size shows that the best solutions obtained are similar for the different sample sizes, but that the mean and the coefficient of variance improve with the initial sample size. We can conclude that the initial sample size that performs best is $N = 50$. For this case, the accuracy of the response surface is within 4.04% and the mean energy of the optimum solutions differ by 9.84% compared to the conventional heuristic optimization, but with a reduction in the computational cost of the 99.06%. Regarding the best solution, the comparison shows that the use of kriging increases the optimum energy by 2.54%. However, if the main objective is to reduce the coefficient of variance, the initial size that performs better is N = 500. For this case, the solutions obtained have a coefficient of variance of 3.67%, even lower than the 3.79% that corresponds to the conventional heuristic optimization. Thus, structural engineers must consider an appropriate initial sample size depending on the characteristics of the problem.

In conclusion, the use of the kriging model in structural design offers a new way to solve a number of structural problems that require a very high computational cost and reduces the difficulty of other problems. On the one hand, due to the lower computational cost, kriging-based heuristic optimization can be used to obtain the best solution for problems involving several criteria and yields robust designs. On the other hand, kriging-based heuristic optimization can be used to optimize structural problems with a lower number of design variables by means of commercial software. In this way, structural engineers can obtain the response objective of a small sample size through commercial software without the necessity of writing code, and after that, achieve an optimized structure in simple terms. Thus, the use of the kriging model in structural design has a high potential in the research field as well as practical engineering.

Acknowledgments

The authors acknowledge the financial support of the Spanish Ministry of Economy and Competitiveness, along with FEDER funding (Project: BIA2017-85098-R).

References

[1] Gervásio H, Simões Da Silva L. A probabilistic decision-making approach for the sustainable assessment of infrastructures. Expert Syst Appl 2012;39:7121–31. https://doi.org/10.1016/j.eswa.2012.01.032.
[2] Aghdaie MH, Zolfani SH, Zavadskas EK. Prioritizing constructing projects of municipalities based on AHP and COPRAS-G: a case study about footbridges in Iran. Balt J Road Bridg Eng 2012;7:145–53. https://doi.org/10.3846/bjrbe.2012.20.
[3] Zavadskas E, Antucheviciene J, Vilutiene T, Adeli H. Sustainable decision-making in civil engineering, construct building technology. Sustainability 2017;10:14. https://doi.org/10.3390/su10010014.
[4] Penadés-Plà V, García-Segura T, Martí J, Yepes V. A review of multi-criteria decision-making methods applied to the sustainable bridge design. Sustainability 2016;8:1295. https://doi.org/10.3390/su8121295.
[5] Ferreiro-Cabello J, Fraile-Garcia E, Martinez-Camara E, Perez-de-la-Parte M. Sensitivity analysis of life cycle assessment to select reinforced concrete structures with one-way slabs. Eng Struct 2017;132:586–96. https://doi.org/10.1016/J.ENGSTRUCT.2016.11.059.
[6] Penadés-Plà V, Martí JV, García-Segura T, Yepes V. Life-cycle assessment: a comparison between two optimal post-tensioned concrete box-girder road bridges. Sustainability 2017;9:1864. https://doi.org/10.3390/su9101864.
[7] Gervasio H, Simoes da Silva L. Comparative life-cycle analysis of steel-concrete composite bridges. Struct Infrastruct Eng 2008;4:251–69. https://doi.org/10.1080/15732470600627325.
[8] Camp CV, Huq F. CO_2 and cost optimization of reinforced concrete frames using a big bang-big crunch algorithm. Eng Struct 2013;48:363–72. https://doi.org/10.1016/j.engstruct.2012.09.004.
[9] Yepes V, Martí JV, García-Segura T. Cost and CO_2 emission optimization of precast-prestressed concrete U-beam road bridges by a hybrid glowworm swarm algorithm. Autom Constr 2015;49:123–34. https://doi.org/10.1016/j.autcon.2014.10.013.
[10] Molina-Moreno F, Martí JV, Yepes V. Carbon embodied optimization for buttressed earth-retaining walls: implications for low-carbon conceptual designs. J Clean Prod 2017;164:872–84. https://doi.org/10.1016/j.jclepro.2017.06.246.
[11] García-Segura T, Yepes V. Multiobjective optimization of post-tensioned concrete box-girder road bridges considering cost, CO_2 emissions, and safety. Eng Struct 2016;125:325–36. https://doi.org/10.1016/j.engstruct.2016.07.012.
[12] Martí JV, García-Segura T, Yepes V. Structural design of precast-prestressed concrete U-beam road bridges based on embodied energy. J Clean Prod 2016;120:231–40. https://doi.org/10.1016/j.jclepro.2016.02.024.
[13] Park H, Kwon B, Shin Y, Kim Y, Hong T, Choi S. Cost and CO_2 emission optimization of steel reinforced concrete columns in high-rise buildings. Energies 2013;6:5609–24. https://doi.org/10.3390/en6115609.
[14] Nigdeli SM, Bekdas G, Kim S, Geem ZW. A novel harmony search based optimization of reinforced concrete biaxially loaded columns. Struct Eng Mech 2015;54:1097–109. https://doi.org/10.12989/sem.2015.54.6.1097.
[15] de Albuquerque AT, El Debs MK, Melo AMC. A cost optimization-based design of precast concrete floors using genetic algorithms. Autom Constr 2012;22:348–56. https://doi.org/10.1016/J.AUTCON.2011.09.013.
[16] García-Segura T, Yepes V, Alcalá J, Pérez-López E. Hybrid harmony search for sustainable design of post-tensioned concrete box-girder pedestrian bridges. Eng Struct 2015;92:112–22. https://doi.org/10.1016/j.engstruct.2015.03.015.
[17] Simpson TW, Booker AJ, Ghosh D, Giunta AA, Koch PN, Yang R-J. Approximation methods in multidisciplinary analysis and optimization: a panel discussion. Struct Multidiscip Optim 2004;27:302–13. https://doi.org/10.1007/s00158-004-0389-9.
[18] Bäckryd RD, Ryberg A-B, Nilsson L. Multidisciplinary design optimisation methods for automotive structures. Int J Automot Mech Eng 2017;14:2229–8649. https://doi.org/10.15282/ijame.14.1.2017.17.0327.
[19] Simpson TW, Poplinski JD, Koch PN, Allen JK. Metamodels for computer-based engineering design: survey and recommendations. Eng Comput 2001;17:129–50. https://doi.org/10.1007/PL00007198.
[20] Cressie N. The origins of kriging. Math Geol 1990;22:239–52. https://doi.org/10.1007/BF00889887.
[21] García-Segura T, Yepes V, Frangopol DM, Yang DY. Lifetime reliability-based optimization of post-tensioned box-girder bridges. Eng Struct 2017;145:381–91.
[22] Kutylowski R, Rasiak B. Application of topology optimization to bridge girder design. Struct Eng Mech 2014;51:39–66. https://doi.org/10.12989/sem.2014.51.1.039.
[23] Martí JV, Yepes V, González-Vidosa F. Memetic algorithm approach to designing

precast-prestressed concrete road bridges with steel fiber reinforcement. J Struct Eng 2015;141:4014114. https://doi.org/10.1061/(ASCE)ST.1943-541X.0001058.
[24] García-Segura T, Yepes V, Frangopol DM. Multi-objective design of post-tensioned concrete road bridges using artificial neural networks. Struct Multidiscip Optim 2017;56:139–50. https://doi.org/10.1007/s00158-017-1653-0.
[25] Barton RR, Meckesheimer M. Metamodel-based simulation optimization. vol. 13; n. d. https://doi.org/10.1016/S0927-0507(06)13018-2.
[26] Myers RH, Montgomery DC, Anderson-Cook CM. Response surface methodology: process and product optimization using designed experiments. Toronto (Canada): Wiley; 1995.
[27] McKay MD, Beckman RJ, Conover WJ. Comparison of three methods for selecting values of input variables in the analysis of output from a computer code. Technometrics 1979;21:239–45. https://doi.org/10.1080/00401706.1979.10489755.
[28] Johnson ME, Moore LM, Ylvisaker D. Minimax and maximin distance designs. J Stat Plan Inference 1990;26:131–48. https://doi.org/10.1016/0378-3758(90)90122-B.
[29] Kalagnanam JR, Diwekar UM. An efficient sampling technique for off-line quality control. Technometrics 1997;39:308. https://doi.org/10.2307/1271135.
[30] Fang K-T, Lin DKJ, Winker P, Zhang Y. Uniform design: Theory and application. Technometrics 2000;42:237. https://doi.org/10.2307/1271079.
[31] Chuang CH, Yang RJ, Li G, Mallela K, Pothuraju P. Multidisciplinary design optimization on vehicle tailor rolled blank design. Struct Multidiscip Optim 2008;35:551–60. https://doi.org/10.1007/s00158-007-0152-0.
[32] Jin R, Chen W, Simpson TW. Comparative studies of metamodelling techniques under multiple modelling criteria. Struct Multidiscip Optim 2001;23:1–13. https://doi.org/10.1007/s00158-001-0160-4.
[33] Li YF, Ng SH, Xie M, Goh TN. A systematic comparison of metamodeling techniques for simulation optimization in decision support systems. Appl Soft Comput 2010;10:1257–73. https://doi.org/10.1016/J.ASOC.2009.11.034.
[34] Kim B-S, Lee Y-B, Choi D-H. Comparison study on the accuracy of metamodeling technique for non-convex functions. J Mech Sci Technol 2009;23:1175–81. https://doi.org/10.1007/s12206-008-1201-3.
[35] Forrester AIJ, Keane AJ. Recent advances in surrogate-based optimization. Prog Aerosp Sci 2009;45:50–79. https://doi.org/10.1016/J.PAEROSCI.2008.11.001.
[36] Matheron G. Principles of geostatistics. Econ Geol 1963;58:1246–66.
[37] Simpson TW, Mauery TM, Korte J, Mistree F. Kriging models for global approximation in simulation-based multidisciplinary design optimization. AIAA J 2001;39:2233–41. https://doi.org/10.2514/3.15017.
[38] Schlaich J, Scheef H. Concrete box-girder bridges. Zürich (Switzerland): Int. Assoc. Bridg. Struct. Eng; 1982.
[39] Catalonia Institute of Construction Technology. BEDEC PR/PCT ITEC material database; 2016.
[40] Ministerio de Fomento. EHE-08: Code on structural concrete. Madrid (Spain); 2008.
[41] Ministerio de Fomento. IAP-11: Code on the actions for the design of road bridges. Madrid (Spain); 2011.
[42] European Committee for Standardization. EN 1001-2:2003. Eurocode 1: Actions on structures – Part 2: Traffic loads bridges. Brussels (Belgium); 2003.
[43] European Committee for Standardisation. EN1992-2:2005. Eurocode 2: Design of concrete structures – Part 2: Concrete Bridge-Design and detailing rules. Brussels; 2005.
[44] Kirkpatrick S, Gelatt CD, Vecchi MP. Optimization by simulated annealing. Science 1983;220:671–80. https://doi.org/10.1126/science.220.4598.671.
[45] Martí JV, González-Vidosa F, Yepes V, Alcalá J. Design of prestressed concrete precast road bridges with hybrid simulated annealing. Eng Struct 2013;48:342–52. https://doi.org/10.1016/j.engstruct.2012.09.014.
[46] Medina JR. Estimation of incident and reflected waves using simulated annealing. J Watery Port Coast Ocean Eng 2001;127:213–21.